

---

---

ELECTRONIC PROPERTIES  
OF SEMICONDUCTORS

---

---

## X-Ray Conductivity of ZnSe Single Crystals

V. Ya. Degoda\* and G. P. Podust

Taras Shevchenko Kyiv National University, Physics Department, Kyiv, 03680 Ukraine

\*e-mail: degoda@univ.kiev.ua

Submitted September 29, 2015; accepted for publication October 7, 2015

**Abstract**—The experimental  $I$ – $V$  and current–illuminance characteristics of the X-ray conductivity and X-ray luminescence of zinc-selenide single crystals feature a nonlinear shape. The performed theoretical analysis of the kinetics of the X-ray conductivity shows that even with the presence of shallow and deep traps for free charge carriers in a semiconductor sample, the integral characteristics of the X-ray conductivity (the current–illuminance and  $I$ – $V$  dependences) should be linear. It is possible to assume that the nonlinearity experimentally obtained in the  $I$ – $V$  and current–illuminance characteristics can be caused by features of the generation of free charge carriers upon X-ray irradiation, i.e., the generation of hundreds of thousands of free charge carriers of opposite sign in a local region with a diameter of  $<1 \mu\text{m}$  and Coulomb interaction between the free charge carriers of opposite signs.

DOI: 10.1134/S1063782616050067

### 1. INTRODUCTION

Zinc selenide (ZnSe) belongs to the most promising wide-gap materials of the  $A^{II}$ – $B^{VI}$  type and is reasonably well investigated [1–3]. ZnSe finds wide application in the fabrication of devices of semiconductor electronics and information-representation systems [4]. To date, it is known that zinc selenide is used in the fabrication of optical lenses, windows, prisms, mirrors, etc., which can operate in the visible and infra-red spectral regions (0.55–22  $\mu\text{m}$ ), in special optical systems, and in  $\text{CO}_2$  lasers.

Over the last decade, one more promising line of application of ZnSe single crystals associated with its use as detectors of ionizing radiation (both indirect (scintillators) [5] and direct conversion of high-energy radiation to an electric current [6, 7]) was developed. In terms of the set of electrical, physical, chemical, and luminescent properties, as well as the radiation resistance, tellurium-doped zinc selenide (ZnSe:Te) is today one of the most efficient scintillators for use in detectors of the “scintillator–photodiode” type [5]. The use of undoped ZnSe as a semiconductor detector became possible only after the development of technologies of the growth of high-quality single crystals with a low concentration of uncontrolled impurities and a high material resistivity of no lower than  $10^{10} \Omega \cdot \text{cm}$ . It is necessary to note that a relatively large value of the effective atomic number  $Z_{\text{ef}} = 32$  and of the band gap  $E_g = 2.7 \text{ eV}$  (at 300 K) make zinc selenide a promising material for the fabrication of X-ray detectors, which require no cooling [6, 7].

In this context, experimental investigations of the X-ray conductivity (XRC) and X-ray luminescence

(XRL) of ZnSe single crystals at various temperatures became a priority. The  $I$ – $V$  and current–illuminance characteristics obtained as a result of carrying out such investigations were found to be nonlinear, with the current–illuminance characteristics of different samples at different temperatures being nonlinear in different ways. This study is devoted to investigating the features of the XRC and XRL characteristics of zinc-selenide single crystals.

### 2. EXPERIMENTAL

The luminescence and conductivity of ZnSe single crystals were investigated upon excitation by X-ray radiation. Zinc-selenide crystals were grown from a preliminarily purified blend, and they were specially undoped during growth. These measures provided the possibility of obtaining samples with the lowest concentration of impurity point defects and with the highest resistivity ( $\rho \geq 10^{12} \Omega \cdot \text{cm}$ ).

To investigate the conductivity, we deposited metallic electric contacts onto the single crystals by the resistive method, to which copper conductors were soldered. For all of the samples, the contacts were represented by rectangular strips 5 mm in length and 1 mm wide. To one electrode, we applied the stabilized voltage from 0 to 1000 V and earthed another electrode via a nanoammeter. The nanoammeter enabled us to measure the value of the current from 1 to 10  $\mu\text{A}$  with an accuracy of 10%, from 10 to 100  $\mu\text{A}$  with an accuracy of 1%, and from 100  $\mu\text{A}$  to 1 mA with an accuracy of  $<1\%$ . For all values of the conduction current, the condition that the input impedance of the nanoammeter be several orders of magnitude lower

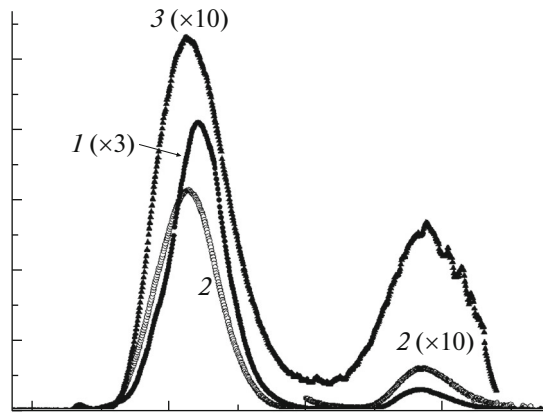


**Fig. 1.** XRL spectra of a ZnSe single crystal as measured at the temperatures (1) 8, (2) 85, and (3) 295 K.

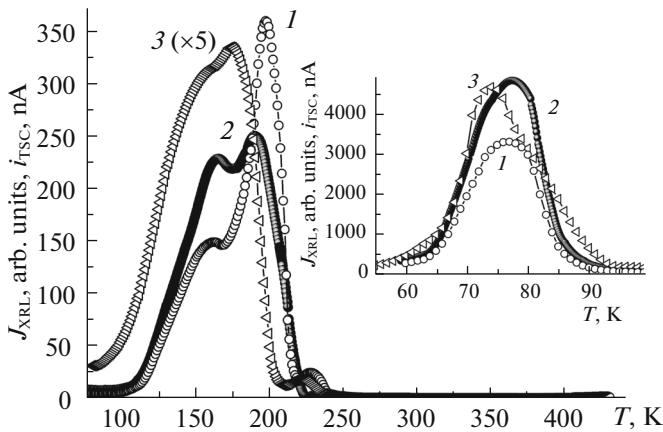


**Fig. 2.** (1, 2) TSL and (3) TSC curves of a ZnSe single crystal after X-ray irradiation (60 min) at 85 and 9 K (in the inset) measured at  $U = 15$  V.

than the electrical resistance of the ZnSe sample was satisfied. Investigations of the conduction current were carried out in vacuum ( $P < 1$  Pa). It was established by the thermopower method that the samples under investigation have  $n$ -type conductivity at room temperature.

When investigating the conductance and luminescence, the sample was placed in a cryostat, which enabled us to use various temperatures in the range from 8 to 500 K. Heating was carried out with the help of a built-in electric heater with a power of up to 800 W, and cooling was carried out with the help of liquid nitrogen or helium.

Comprehensive experimental investigations of the dark and X-ray conductivities and the X-ray luminescence at various temperatures, the thermally stimulated conductivity (TSC) and thermally stimulated luminescence (TSL), the TSL and TSC dose dependences, the phosphorescence and the current relaxation (CR), the  $I$ - $V$  characteristic and current-illumination

dependences for the X-ray conductivity and the X-ray luminescence were carried out.

The X-ray luminescence and the X-ray conductivity were excited at normal incidence of integral radiation on the sample surface from an X-ray tube BKhV-7 (Re, 20 kV, 5–25 mA, and  $L = 130$  mm) through a beryllium window in the cryostat. The X-ray-excitation intensity was varied by changing the anode current of the X-ray tube at a constant voltage. In this case, the shape of the radiation spectrum of the X-ray tube is not changed, and the X-ray-radiation intensity was proportional to the value of the anode current of the tube. The optical axis of the detection system passed in between the electrical contacts at an angle of  $45^\circ$  to the normal to the sample surface, which was uniformly irradiated with X-ray photons. To detect the X-ray luminescence, we used two channels: integral and spectral. When using the integral channel, the luminescence radiation was focused with the help of a quartz lens onto the photocathode of the photoelectric multiplier (PMT-106). For spectral detection, we used a wide-aperture monochromator MDR-2 (diffraction grating with 600 grooves per mm) and two detectors: PMT-106 (400–820 nm) or cooled PMT-83 (600–1200 nm). The accuracy in determining the X-ray-luminescence intensity was no lower than 3% and was limited by the presence of the PMT “dark” currents and detection-system noise. All spectral dependences presented in this study are corrected to the spectral sensitivity of the recording system. The experimental current–luminescence dependences of the luminescence and the conductivity were measured in two modes: decreasing (25  $\rightarrow$  5 mA) and increasing (5  $\rightarrow$  25 mA) X-ray radiation intensity. At an irradiation duration exceeding 3 min for each value of the excitation intensity, there is almost no difference in the current–luminescence curves for both modes.

### 3. RESULTS OF EXPERIMENTAL INVESTIGATIONS

#### 3.1. XRL Spectra, TSL and TSC of Zinc-Selenide Single Crystals

The typical XRL spectra for ZnSe single-crystal samples in the range from 400 to 1200 nm at various temperatures are shown in Fig. 1. The spectra of various high-resistivity samples differ only in the relation between the intensities of the two main luminescence bands with peaks at 630 and 970 nm. According to [1, 8], the band at 630 nm is caused by a complex center including a zinc vacancy, and the band with a peak at 970 nm is caused by a complex center with a selenium vacancy or a copper impurity [9, 10].

These XRL bands are caused by the luminescence-recombination mechanism because they are observed in the phosphorescence and the TSL. In Fig. 2, we show the characteristic TSL curves for the case of recording the 630- and 970-nm bands and the TSC of

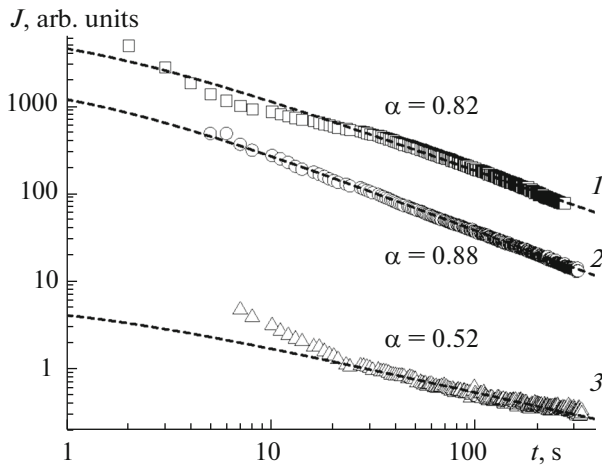


Fig. 3. Phosphorescence of a ZnSe single crystal after X-ray excitation at  $T = (1)$  9,  $(2)$  85, and  $(3)$  295 K.

one of the ZnSe samples. In all investigations of the luminescence for the 970-nm band, recording was carried out at a wavelength of 953 nm because the real peak (without taking into account the spectral sensitivity of the system) is observed exactly at this wavelength.

The TSL and TSC curves are accurately recorded in all samples under investigation and testify to an appreciable level of storage of nonequilibrium charge carriers in traps. The largest fraction of carriers is delocalized thermally from the traps upon heating to a temperature of 250 K, which testifies to the dominance of shallow traps in the material under investigation.

The absence of light-sum accumulation at deep traps at room temperature is confirmed also by the absence of appreciable phosphorescence at this temperature (Fig. 3, curve 3). At low temperatures (9 and 85 K), significant phosphorescence (Fig. 3, curves 1 and 2) is observed, which testifies to the presence of the array of traps located at various depths. The curve of phosphorescence decay and the conduction-current relaxation are well approximated by hyperboles in the time interval to 500 s and described by the phenomenological Becquerel dependence [11, 12]:

$$I_{\text{ph}}(t) = \frac{I_0}{(1 + a \cdot t)^\alpha}, \quad \alpha \leq 2.$$

The hyperbole index  $\alpha$  for high irradiation doses attains values of  $\alpha_{\text{ph}} = 0.88$  for the phosphorescence and  $\alpha_{\text{RC}} = 0.89$  for the RC (i.e.,  $\alpha_{\text{ph}} < \alpha_{\text{RC}}$ ), which contradicts the classical kinetic theory of photoluminescence [12–14] and photoconductivity [15–18].

It should be noted that the sensitivity of the recording system for detection of the TSL, TSC, CR, and phosphorescence was increased by several orders of magnitude in comparison with the steady-state luminescence and conductivity.

Using four values of temperature (9, 85, 295 and 400 K) for the investigations, we have principally different relations between the concentrations of shallow and deep traps. At liquid-helium temperatures, almost all of the traps are deep. With increasing temperature to  $T = 85$  K, the number of shallow traps increases so that their effect on the XRL and XRC kinetics becomes substantial. At room temperature, only a small fraction of traps remain deep, the majority of them become shallow, and the deep-trap concentration decreases upon further heating of the sample, while there are only shallow traps for free charge carriers at  $T > 400$  K.

Thus, fundamentally different cases are implemented at low and high temperatures: at  $T \leq 10$  K, it is mainly deep traps for free charge carriers that affect the XRL and XRC kinetics; at an increase in the temperature, the contribution of shallow traps to the XRL and XRC kinetics becomes more and more substantial, and the XRL and XRC kinetics depends only on shallow traps at high temperatures ( $T > 400$  K).

### 3.2. $I$ – $V$ Characteristics of the X-Ray Conductivity

The  $I$ – $V$  characteristics of the X-ray conductivity of several ZnSe single-crystal samples were investigated at temperatures of 9, 85, 295, and 400 K and at various X-ray-tube currents  $I_T = 5, 15, \text{ and } 25$  mA.

In all samples under investigation, the  $I$ – $V$  characteristics of the X-ray conductivity at various temperatures feature superlinear behavior and are well approximated by a power function with the exponent  $\alpha > 1$ , which varies with temperature. For all samples, the  $I$ – $V$  characteristics of the XRC at  $T > 400$  K are almost linear with the exponent  $\alpha = 1.04$ – $1.09$ . The  $I$ – $V$  characteristics of the XRC measured at room temperature are already notably superlinear, and  $\alpha$  varies within the limits of 1.2–1.3. At low temperatures, the  $I$ – $V$  dependences become even more superlinear,  $\alpha > 1.4$ , and the dependence  $i_{\text{XRC}}(U)$  becomes even square-law at liquid-helium temperatures ( $T < 10$  K) in some samples. Thus, a natural increase in the degree of superlinearity is observed with decreasing temperature in all samples under investigation. The typical  $I$ – $V$  dependences of the XRC current for a ZnSe single crystal are shown in Fig. 4.

It is necessary also to note the presence of the effect of an external electric field on the steady-state XRL intensity. A linear decrease in the XRL intensity is experimentally observed with increasing field from 0 to 2000 V/cm; this decrease reaches 13% for the XRL intensity at a radiation wavelength of 630 nm.

### 3.3. Current–Illuminance Characteristics of XRC and XRL

The current–illuminance characteristics of the XRC measured at various temperatures in all samples

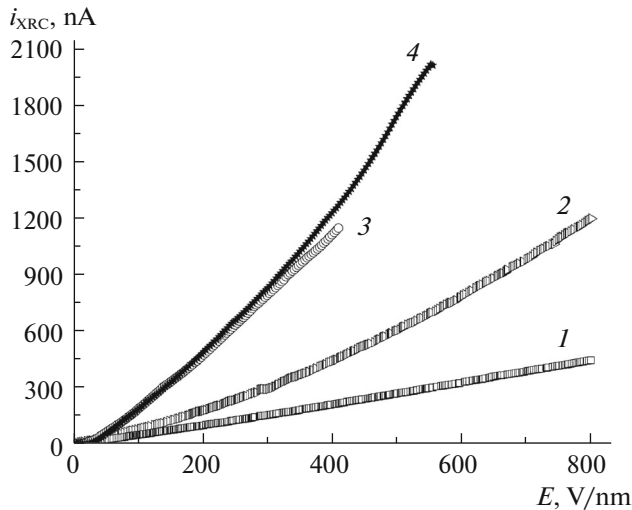


**Fig. 4.**  $I$ - $V$  characteristics for the X-ray conductivity of a ZnSe single-crystal sample at the temperatures  $T = (1)$  407 ( $\alpha = 1.1$ ),  $(2)$  295 ( $\alpha = 1.29$ ),  $(3)$  85 ( $\alpha = 1.31$ ), and  $(4)$  9 ( $\alpha = 1.41$ ) K.

under investigation have a nonlinear character and are also well approximated by a power function with the exponent  $\beta$  (Figs. 5 and 6). The current–illuminance characteristics of the conductivity measured at high temperatures ( $T = 400$ – $410$  K) have a sublinear character with  $\beta = 0.8$ – $0.9$ . At room temperature, the current–illuminance characteristics of the XRC have a similar high-temperature character in some samples, are highly superlinear in others, and even attain a value of  $\beta = 1.4$ . The current–illuminance characteristics of the XRC have a sublinear character with  $\beta = 0.6$ – $0.9$  at 85 K and are superlinear with  $\beta = 1.43$  only for one sample. The measured current–illuminance characteristics of the XRC of the same sample at 9 K remain sublinear with  $\beta = 0.69$ .

The current–illuminance characteristics of the XRL at a radiation wavelength of 630 nm are almost linear ( $\beta$  does not differ much from unity), the exponent  $\beta$  either increasing or decreasing with temperature in the range  $\beta = 0.95$ – $1.10$  depending on the sample. The current–illuminance characteristics of the XRL at a radiation wavelength of 970 nm have a similar shape, only  $\beta > 1$  is always observed. Only one sample for which the dependence  $\beta(T)$  has a peak (different for two luminescence bands) is an exception.

Comparing the intensities of the XRL current–illuminance characteristics for two luminescence bands of various ZnSe samples at different temperatures, we found that they do not intersect each other. The more intense band remains the most intense at all excitation levels and all temperatures. In this case, the intensities of the TSL peaks at the largest irradiation dose are close in magnitude upon the recording of different luminescence bands. In general, no correlation of the current–illuminance characteristics at two

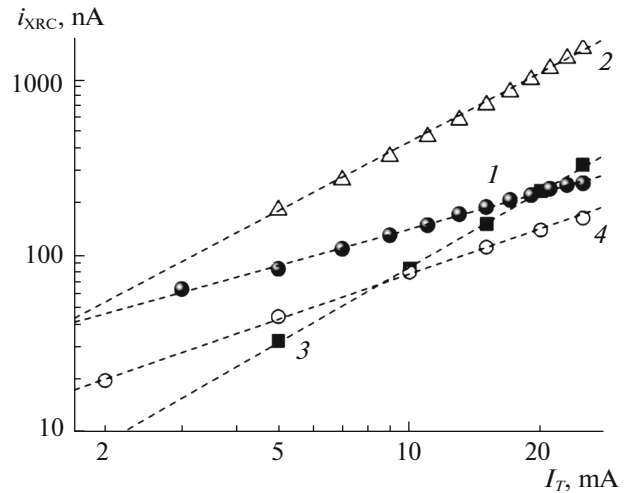


**Fig. 5.** Current–illuminance characteristics of the X-ray conductivity for a ZnSe single-crystal sample at temperatures of  $T = (1)$  9 ( $\beta = 0.69$ ),  $(2)$  85 ( $\beta = 1.31$ ),  $(3)$  295 ( $\beta = 1.43$ ), and  $(4)$  407 ( $\beta = 0.86$ ) K.

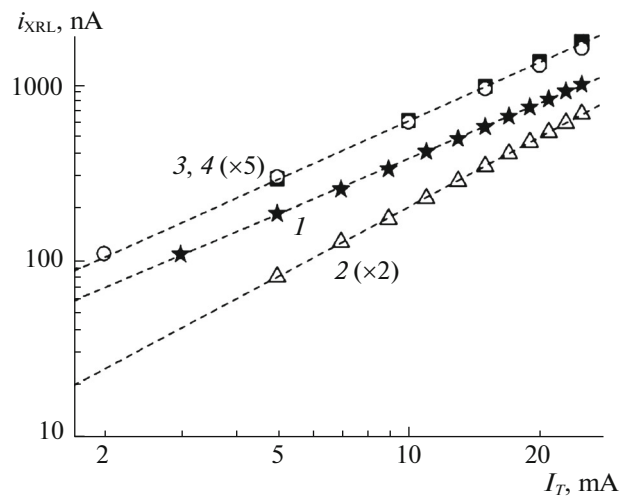


**Fig. 6.** Current–illuminance characteristics for the X-ray luminescence of a ZnSe single-crystal sample at a radiation wavelength of 630 nm at temperatures of  $T = (1)$  9 ( $\beta = 1.05$ ),  $(2)$  85 ( $\beta = 1.32$ ),  $(3)$  295 ( $\beta = 1.11$ ), and  $(4)$  407 ( $\beta = 1.06$ ) K.

luminescence bands (630 and 970 nm) was found, but the most important fact is that the majority of them do not differ significantly from linear dependences in the entire temperature range of 8–500 K.

#### 4. THEORETICAL ANALYSIS OF THE X-RAY-CONDUCTIVITY KINETICS

The obtained experimental  $I$ - $V$  and current–illuminance characteristics, as well as the phosphorescence and CR curves for the X-ray luminescence and

X-ray conductivity of ZnSe crystals cannot be explained within the framework of classical kinetic theories of photoluminescence [12–14] and photoconductivity [15–18]. Classical theory considers the fundamental model of a semiconductor with one type of trap and one type of recombination (luminescence) center. In this case, the free charge-carrier concentrations ( $N^-$ ,  $N^+$ ) and the charge-exchange luminescence-center concentration ( $n_j$ ) for the steady state are proportional to the root of the excitation intensity:  $N^-$ ,  $n_j \sim \sqrt{I_{\text{ex}}}$ . As a result, we have the linear dependences ( $I_{\text{lum}} \sim N^- \cdot n_j \sim I_{\text{ex}}$ ) for the current–illumination characteristic of the luminescence ( $I_{\text{lum}}$ ). Correspondingly, the steady-state free-charge-carrier concentration is independent of the applied electric field, and the  $I$ – $V$  characteristics should have a linear shape (i.e., Ohm's law should be fulfilled). After X-ray-excitation is stopped, we detected attenuation of the phosphorescence and CR. Since the intensity of the phosphorescence, which is related to recombination luminescence, is also proportional to the product  $\{I_{\text{ph}} \sim N^-(t)n_j(t)\}$  of the free-charge-carrier concentration and the concentration of charge–exchange recombination centers at each moment of time (both concentrations decreasing during phosphorescence), and the current relaxation is proportional only to the free-charge-carrier concentration  $\{i_{\text{RC}} \sim N^-(t)\}$ , the phosphorescence should decay faster than the CR. Experimentally, we have  $\alpha_{\text{ph}} < \alpha_{\text{RC}}$ .

Therefore, detailed analysis of the model of crystal phosphors was carried out with three types (shallow, phosphorescent, and deep) of traps and with two centers of recombination. The probability  $w_i$  of charge-carrier delocalization from a trap is determined [12–18] as:

$$w_i = w_{0i} \exp\left(-\frac{E_i}{kT}\right), \quad (1)$$

where  $w_{0i}$  is the frequency factor (caused by the trap nature),  $E_i$  is the depth of the level in the band gap,  $k$  is the Boltzmann constant, and  $T$  is the sample temperature. As the shallow trap, we consider a trap at temperature  $T$  for which  $w_i > 1 \text{ s}^{-1}$ ; a phosphorescent trap is considered to be a trap with  $w_i < 1 \text{ s}^{-1}$  (i.e., does not greatly differ from  $1 \text{ s}^{-1}$ ); and a deep trap, a trap with  $w_i \ll 1 \text{ s}^{-1}$ . To take into account the spatial distribution of X-ray-radiation absorption in the sample, it is expedient to divide it into layers with a thickness, which is slightly larger than the diffusion expansion for the longest drift time. The set of kinetic equations for such a semiconductor model consists of eight differential equations:

- (i) for free electrons;
- (ii) for free holes;
- (iii) for electrons localized at shallow traps;

- (iv) for electrons localized at the phosphorescent trap;
- (v) for electrons localized at deep traps;
- (vi) for holes localized at the first luminescence center;
- (vii) for holes localized at the second luminescence center; and
- (viii) the balance equation for charge carriers with different signs.

It is possible to find an approximate solution in the analytical form for the steady state and to obtain the dependences of all concentrations of charge carriers on the excitation intensity. As a result, we obtain for the free-carrier concentration

$$N_{\infty}^- = \tau_0^- \left( N_G + w \frac{v_i v_j}{v_i + v_j} \right), \quad N_{\infty}^- = \tau_0^+ N_G, \quad (2)$$

where  $N_G$  is the concentration of generated electron–hole pairs;  $\tau_0^-$  and  $\tau_0^+$  are the lifetimes of free electrons and holes in the bands;  $v_{(i-1)}$ ,  $v_i$ ,  $v_{(i+1)}$ , and  $v_j$  are the concentrations of shallow, phosphorescent, and deep traps, and the luminescence centers. For concentrations of charge carriers localized at shallow traps, we have

$$n_{(i-1)\infty} = N_{\infty}^- \frac{v_{(i-1)}}{N_C} \exp\left(\frac{E_{(i-1)}}{kT}\right), \quad (3)$$

$$N_C = 2 \left( \frac{2\pi m_e kT}{h^2} \right)^{\frac{3}{2}},$$

where  $N_C$  is the effective density of states of electrons in the conduction band. For electrons localized at deep traps and holes localized at luminescence centers

$$n_{(i+1)\infty} = \frac{v_{(i+1)}v_j}{(v_i + v_{(i+1)})g + v_j}, \quad (4)$$

$$n_{j\infty} = \frac{v_j(v_i + v_{(i+1)})}{(v_i + v_{(i+1)}) + v_j g},$$

where the dimensionless parameter  $g$  is determined by the ratio of the concentrations of generated and delocalized electrons to the concentration of generated electrons:

$$n_{i\infty} = \frac{v_i v_j}{\left( \frac{v_i + v_{(i+1)}}{g} \right) \left( 1 + \frac{w_i v_j}{N_G} \right) + v_j}. \quad (5)$$

Thus, for the steady state, the concentration of charge carriers at shallow traps is much lower than the corresponding concentrations at the phosphorescent and deep traps, the degree of occupation of the latter traps being independent of the excitation intensity. The degree of occupation of phosphorescent traps depends only slightly on  $N_G(I_{\text{ex}})$ , and the steady-state concentration of free charge carriers in the band is propor-

tional to the excitation intensity. Thus, expansion of the semiconductor model changes the dependences of the concentration of free and localized charge carriers, as well as the concentrations of recharged luminescence centers on the intensity of the excitation radiation, but the current–illuminance  $I$ – $V$  characteristics should remain linear.

Since it is homogeneous excitation that is used for these models (the classical and considered), and the experimental results were obtained for X-ray irradiation, it is necessary to take into account micro-inhomogeneous excitation of the semiconductor upon the absorption of one X-ray photon.

## 5. ANALYSIS OF THE EXPERIMENTAL RESULTS

The experimental  $I$ – $V$  and current–illuminance dependences, as was already mentioned, are nonlinear. For optical band-to-band excitation (photoexcitation), the current–illuminance dependence  $J_{\text{lum}} \propto J_{\text{ex}}$  of the luminescence should be linear according to classical kinetic theory of photoluminescence, [12–14]. The current–illuminance dependences of the photoconductivity should be proportional to the intensities at a power of 1/2; i.e.,  $i \propto \sqrt{J_{\text{ex}}}$  according to the classical kinetic theory of photoconductivity [15–18]. X-ray excitation differs from optical excitation in that the X-photon energy is a thousand times higher than the band gap of the material ( $E_g$ ), and  $N_0 = h\nu_X/3E_g$  free electron–hole pairs are generated upon the absorption of one photon ( $h\nu_X$ ). The superlinearity of the current–illuminance characteristic for the XRC current contradicts the classical kinetic theory of photoconductivity. This means that the dominant conductivity processes upon X-ray excitation are not the same that are dominant in the photoconductivity.

It could be possible to relate the nonlinearity of the current–illuminance characteristics to the X-ray-tube characteristics. However, it is known that the radiation intensity of the X-ray tube is determined as  $I_X = BI_A U_A^2$ , where  $B$  is the constant coefficient for each type of tube,  $I_A$  is the anode current, i.e., linearly depends on the anode current. In addition, the nonlinearity of the current–illuminance curves is specific for different samples and, thus, it is caused by physical processes in the sample material instead of by the experimental apparatus.

The measured  $I$ – $V$  characteristics of ZnSe single crystals at various values of the X-ray-tube current showed that a variation in the excitation intensity also affects the exponent  $\alpha$ . For detailed consideration of the effect of an increase in  $I_T$  on the shape of the curves of the  $I$ – $V$  characteristics, we investigated the dependences of the ratios  $i_1/i_2$  of the XRC currents on the voltage for different excitation intensities  $I_{T1} > I_{T2}$  and at various temperatures. It was found that the rela-

tion between the XRC currents fits well with a straight line, the slope of these straight lines always increases with the ratio of excitation intensities. However, this increase is small: at a slope coefficient of  $\sim 10^{-4}$ , the variation amounts to several ten-thousandths.

The change in the shape of the curves of the  $I$ – $V$  characteristics is well correlated with the behavior of the current–illuminance characteristics. In the samples with superlinear current–illuminance characteristics, the exponent  $\alpha$  increases with intensity, and we have a decrease in  $\alpha$  with an increase in the excitation intensity ( $I_T$ ) in samples with sublinear current–illuminance characteristics.

## 6. CONCLUSIONS

The general shape of the  $I$ – $V$  dependences for the X-ray conductivity of ZnSe single crystals is superlinear, with the degree of superlinearity increasing with temperature. The overwhelming majority of the current–illuminance characteristics are also nonlinear. The temperature variation, i.e., the change in the relation between the number of shallow and deep traps differently affects the shape of the current–illuminance and  $I$ – $V$  characteristics. It is quite obvious that the nonlinearities of the current–illuminance and  $I$ – $V$  characteristics have a different physical nature and are caused by various physical processes.

The results of comprehensive investigation of the X-ray luminescence and the X-ray conductivity of several single crystal samples of zinc selenide showed that the deep traps affect the XRL kinetics and XRC kinetics, first of all, changing the concentration of localized charge carriers.

Theoretical consideration of the XRC kinetics for the simplified model of a semiconductor showed that, even at the presence of shallow and deep traps for free carriers, the integrated XRC characteristics (the  $I$ – $V$  characteristic, the current–illuminance characteristic) should be linear. Therefore, it is possible to assume that the superlinearity of the experimentally obtained  $I$ – $V$  characteristics is caused by the pronounced effect of micro-inhomogeneity in the generation of free charge carriers upon the absorption of X-ray photons, i.e., is caused by the excitation characteristics themselves.

## REFERENCES

1. D. D. Nedeoglo and A. V. Simashkevich, *Electric and Luminescence Properties of Zinc Selenide* (Kishinev, Shtiintsa, 1984) [in Russian].
2. A. N. Georgobiani and M. K. Sheinkman, *Physics of II–VI Compounds* (Nauka, Moscow, 1986) [in Russian].
3. *Optical Properties of Semiconductors: A Handbook*, Ed. by V. I. Gavrilenko, A. M. Grehov, D. V. Korbutiak, and V. G. Litovchenko (Nauk. Dumka, Kiev, 1987) [in Russian].

4. N. K. Morozova and V. A. Kuznetsov, *Zinc Sulfide: Preparation and Optical Properties* (Nauka, Moscow, 1992) [in Russian].
5. L. V. Atroshchenko, S. F. Burachas, L. P. Gal'chinetskii, B. V. Grinev, V. D. Ryzhikov, and N. G. Starzhinskii, *Scintillator Crystals and Ionizing-Radiation Detectors on their Basis* (Nauk. Dumka, Kiev, 1998) [in Russian].
6. A. O. Sofiienko and V. Y. Degoda, *Rad. Meas.* **47**, 27 (2012).
7. M. S. Brodyn, V. Ya. Degoda, A. O. Sofiienko, B. V. Kozhushko, and V. T. Vesna, *Rad. Meas.* **65**, 36 (2014).
8. V. D. Ryzhikov, *Scintillator Crystals of Semiconductor II–VI Compounds* (NIITEKhIM, Moscow, 1989) [in Russian].
9. N. K. Morozova, I. A. Karetnikov, V. V. Blinov, and E. M. Gavrishchuk, *Semiconductors* **35**, 512 (2001).
10. A. P. Okonechnikov, Extended Abstract of Doctoral Dissertation (Ekaterinburg, 1996).
11. V. Ya. Degoda, *Principles of Photoelectrical-Phenomena Kinetics in Crystal Phosphores* (Kiev. Univ., Kiev, 2009) [in Ukrainian].
12. E. I. Adirovich, *Some Topics in the Theory of the Luminescence of Crystals* (GITTL, Moscow, 1956) [in Russian].
13. M. V. Fok, *Introduction to the Kinetics of Luminescence of Phosphorescent Crystals* (Nauka, Moscow, 1964) [in Russian].
14. A. I. Anselm, *Introduction to Semiconductor Theory* (Prentice-Hall, Englewood Cliffs, 1981; Nauka, Moscow, 1978).
15. V. V. Antonov-Romanovskii, *Kinetics of Luminescence of Phosphorescent Crystals* (Nauka, Moscow, 1966) [in Russian].
16. R. H. Bube, *Photoconductivity of Solids* (Krieger, New York, 1978).
17. S. M. Ryvkin, *Photoelectric Phenomena in Semiconductors* (Fizmatgiz, Moscow, 1963) [in Russian].
18. S. Datta, *Quantum Transport: Atom to Transistor* (Cambridge Univ. Press, New York, 2005).

*Translated by V. Bukhanov*